

Analysis of Malfunction of Robot by ESD using Optical Electric Field Sensor

Takayoshi Ohtsu^{1*}, Yuma Nagao¹ and Ryuji Ohsawa²

¹Department of Electrical and Electronic Engineering, National Institute of Technology, Numazu College, Japan

²SEIKOH GIKEN Co.,Ltd. Ooka, Numazu, Shizuoka, Japan

Abstract

Due to the decrease in the electrostatic strength of electronic devices, there is concern about the effects of transient changes in the electromagnetic field on them. The optical voltage probe has high input impedance, can observe the signal waveform without affecting the circuit, and has little influence on the system to be measured by using the optical fiber cable. Furthermore, since the frequency characteristics are flat, it is possible to measure the original waveform with an oscilloscope. Therefore, the malfunction of the robot due to electrostatic discharge was analyzed using an optical voltage probe.

Keywords: ESD • Optical voltage probe • Malfunction • Robot

Introduction

As the performance and density of electronic devices increase, the mounting density of wiring is increasing, the frequency is increasing and the bandwidth is increasing. Therefore, the robustness of electrostatic discharge is reduced, and countermeasures are required. In addition, while it has the advantage of being able to make the device smaller, it has the disadvantage of being vulnerable to electrostatics. Therefore, the demand for reliability of electronic devices is increasing, such as the loss of important information due to electrostatic destruction and the lack of safety due to malfunction [1-7]. In previous studies, measurements and simulations have been performed on malfunctions caused by the application of electrostatics to the control board of a robot. As a result, it was found that the malfunction of the robot occurs at a voltage of 5 V or less [8]. When observing the waveform on the circuit board, there is a concern that the impedance of the measurement probe may affect the waveform. Therefore, in this study, we used a voltage probe (hereinafter referred to as an optical electric field probe) that uses an optical voltage sensor that can measure with high accuracy even at a voltage of 5 V or less. By attaching an optical voltage probe to the control board of the robot and measuring the malfunction caused by the application of electrostatics, the mechanism of the malfunction will be elucidated.

Experimental Methods

The optical voltage probe controller (SEIKOH GIKEN) used in this experiment is shown in **Figure 1**, and the optical voltage probe head (C1 & OVA6S) is shown in **Figure 2**.

The optical voltage probe uses a thin film type EO crystal (electro-optical crystal) that utilizes the Pockels effect, which changes the refractive index when a voltage is applied. In addition, a Mach-Zehnder interferometer is formed as a waveguide to achieve high sensitivity over a wide band.

Figure 3 shows a malfunction test robot using a Studuino. The Studuino

***Address for Correspondence:** Takayoshi Ohtsu, Department of Electrical and Electronic Engineering, National Institute of Technology, Numazu College, Japan, E-mail: ohtsu@numazu-ct.ac.jp

Copyright: © 2021 Ohtsu T, et al. This is an open-access article distributed under the terms of the Creative Commons Attribution License, which permits unrestricted use, distribution, and reproduction in any medium, provided the original author and source are credited.

Received 15 September 2021; **Accepted** 30 September 2021; **Published** 07 October 2021

(manufactured by Artec) is an Arduino compatible board equipped with a control microcomputer, a motor driver IC, and input / output ports for servo motors, DC motors, and sensors. The Arduino is the simplest board for digital control, consumes very little power, is also open source hardware, and is spreading worldwide not only for educational institutions, but also for hobby and enterprise. Therefore, the reliability of electronic systems using an Arduino is required. Among the Arduino compatible boards, the Studio is suitable for malfunction analysis because it cooperates with Artec and the circuit diagram is presented.

The optical voltage probe head was soldered to the reset terminal and ground of the Studio board, and the applied voltage at the time of contact discharge to the USB port and air discharge and the peak value, half width, and zero cross time of the input waveform were compared. The applied voltage of the ESD gun is shown in **Table 1**.

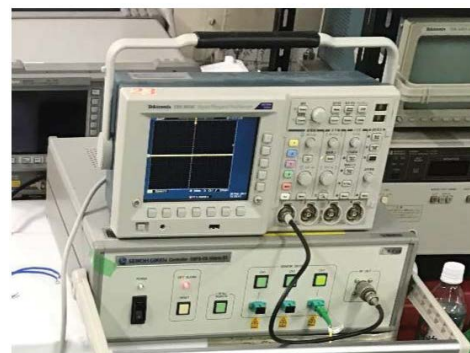


Figure 1. Optical voltage probe controller.



Figure 2. Optical Voltage head.

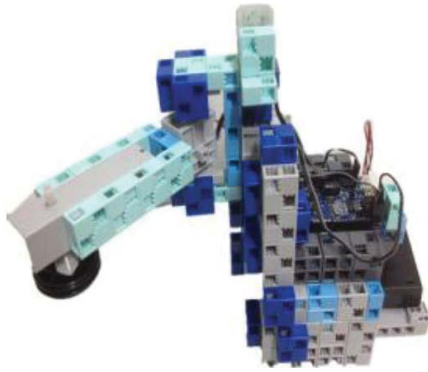


Figure 3. Malfunction test robot.

Table 1: Applied voltage of the ESD gun.

No	Voltage
1	0.2
2	0.3
3	0.5
4	0.8
5	1.0
6	2.0
7	3.0
8	5.0
9	8.0
10	10.0
11	15.0

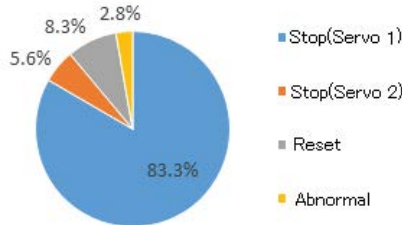


Figure 4. Malfunction mode.

Experimental Results & Consideration

A. Malfunction mode and reset terminal input waveform

Figure 4 shows the breakdown of the observed malfunction modes. The following four types of malfunctions were observed due to the application of ESD.

1. Servo 1 stops in servo 1 stop mode.
2. Servo 2 stops in servo 2 stop mode.
3. Reset mode in which the servo motor returns to the origin.
4. Abnormal operation mode operates abnormally.

In addition, the probability of reset mode and stop mode occurring among all malfunctions was 93%. It was found that both the reset mode and the stop mode are phenomena that occur at the voltage that enters the reset terminal.

Figure 5 shows a typical waveform observed at the reset terminal using an optical voltage probe. It was found that a waveform with amplitude of several V was applied to the reset terminal due to the discharge by the ESD gun to the USB terminal. The zero cross time, peak value, and full width at half maximum were calculated in order to examine the relationship with the malfunction of the robot.

B. Dependence of malfunction occurrence rate on applied voltage

Figure 6 shows the dependence of the malfunction rate on the applied voltage. It was found that the larger the applied voltage for both contact discharge and air discharge, the higher the malfunction rate, and that both contact discharge and air discharge malfunction after exceeding 8 kV.

C. Dependence of peak value on applied voltage

Figure 7 shows the comparison result of the applied voltage dependence of the peak value. In both contact discharge and air discharge, the peak value increases as the applied voltage increases, but it shows an almost constant value near -7 V. It is considered that this is due to the protection circuit of the Studuino board used in the experiment. In addition, the contact discharge is -7V at a lower applied voltage than the air discharge.

D. Dependence of half-value width applied voltage

Figure 8 shows the comparison result of the application voltage dependence of the half-value width. It was found that the half-value width increases when the applied voltage is increased from 0 to 2 kV, but the slope decreases when the applied voltage is 2 kV or more.

E. Comparison of zero crossing time

Figure 9 shows the observation waveforms at + 8kV, + 14kV, and + 20kV. (a) is the case where there is no malfunction at + 8kV, (b) is the case where it malfunctions at + 14kV (stop mode), and (c) is the case where it malfunctions at + 20kV (stop mode). Although there is no significant difference in the peak

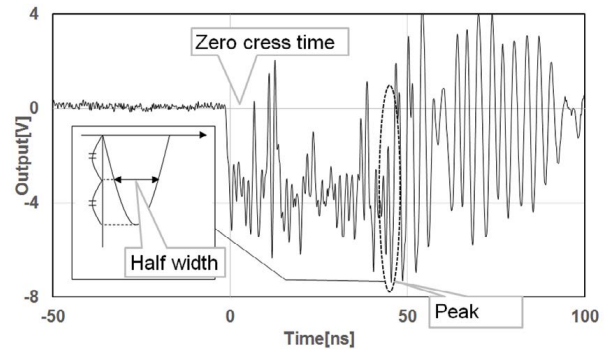


Figure 5. Definition of Peak, half width and zero cross time.

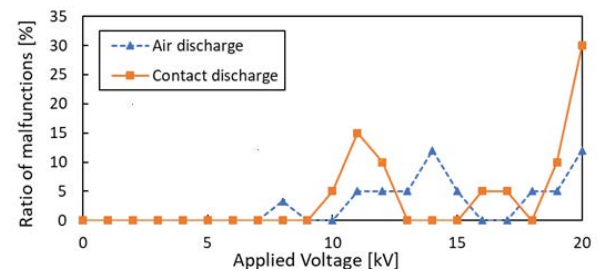


Figure 6. Ratio of malfunction.

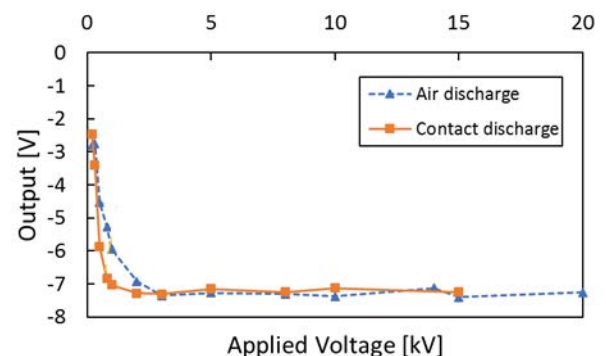


Figure 7. Peak vs. Applied voltage.

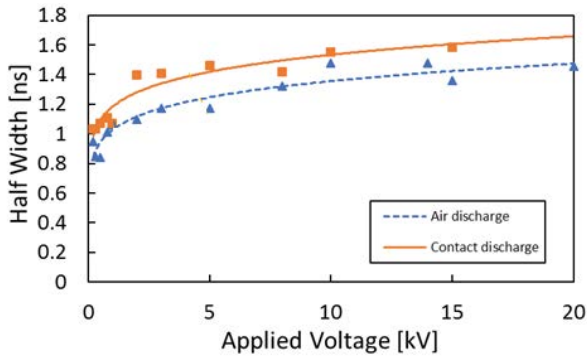


Figure 8. Half width vs. applied voltage.

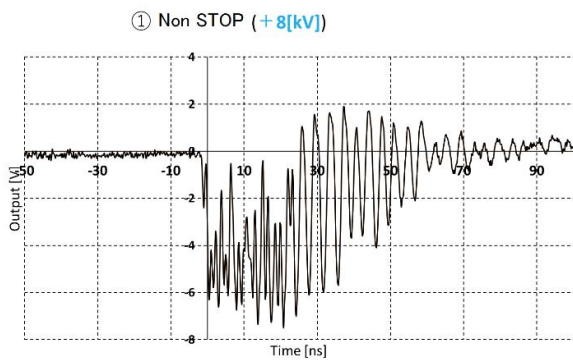


Figure 9 (a). Non STOP +8kV.

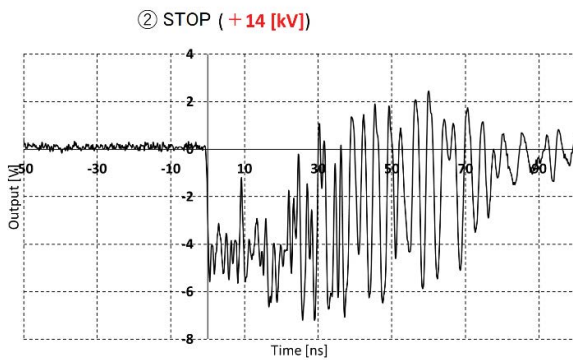


Figure 9 (b). STOP mode +14kV.

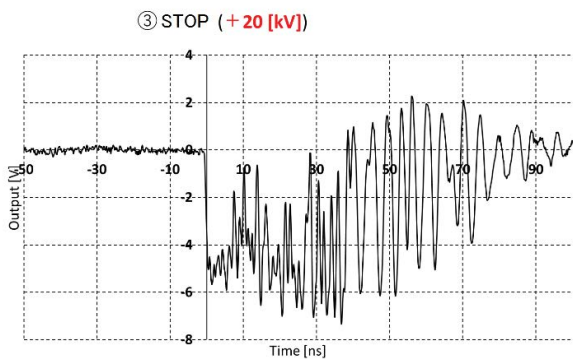


Figure 9 (c). STOP mode +20kV.

value from these, it can be seen that the larger the applied voltage, the longer the zero cross time.

Figure 10 shows the applied voltage dependence of the first peak, the second peak, and the third peak. From this, it was found that the time to the first peak, the second peak, and the third peak becomes longer when the applied voltage is increased.

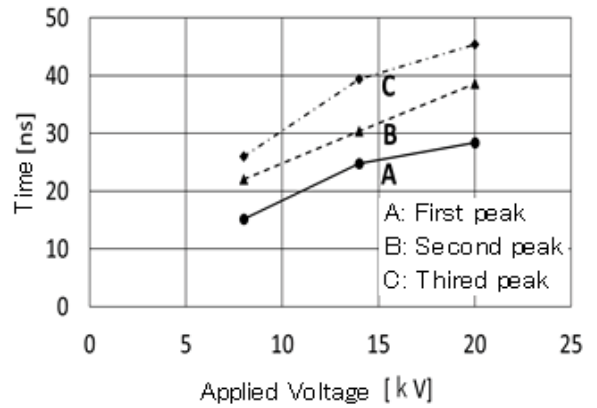


Figure 10. Peak time vs. applied voltage.

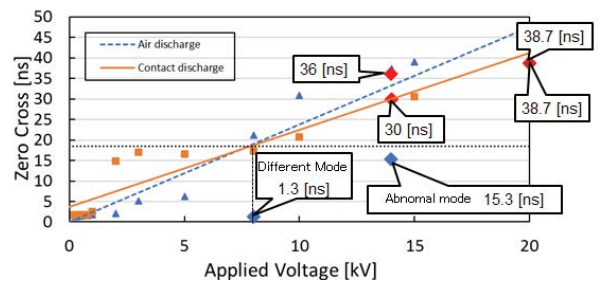


Figure 11. Zero cross time vs. applied voltage.

F. Zero cross time and malfunction

Figure 11 shows the result of the applied voltage dependence of zero cross time. The solid line is for contact discharge, and the dotted line is for air discharge. It was found that the zero cross time increases as the applied voltage increases in both the contact discharge and the air discharge. In addition, 6 points that corresponded to the malfunction and the waveform were plotted in the figure. The intersection of 8 kV where the malfunction started and the zero crosses time was 18.5 ns. If a waveform with a zero crosses time of 18.5 ns or more is input to the Stud no board, it is considered that a malfunction of the reset mode and stop mode is likely to occur. Therefore, it was found that 67% of the malfunctioning waveforms had a zero cross time of more than 18.5 ns.

Conclusion

Using an optical voltage probe using an optical electric field sensor, the malfunction waveform of the robot using Studino was observed, and the following was clarified.

1. In the breakdown of malfunctions, the probability that reset mode and stop mode will occur is 93 %, which is due to an abnormal signal to the reset terminal.
2. The malfunction probability increases when both contact discharge and air discharge exceed 8 kV.
3. Since the change in the peak value and full width at half maximum of the waveform at the applied voltage of 8 kV or higher is small, it is considered that the relationship with the malfunction is low.
4. The zero cross time has a linear characteristic that becomes longer when it is increased with the applied voltage. Since the larger the applied voltage is, the more likely it is that a malfunction will occur. Therefore, it is considered that the larger the zero crosses time, the more likely the malfunction will occur.
5. 67 % of the waveform that actually malfunctioned has a zero cross time exceeding 18.5 ns, and the waveform that malfunctioned has a long zero cross time.

References

1. Tian, Hong, and Lee J.J.K. "Electrostatic discharge damage of MR heads." *IEEE Trans Magn* 31 (1995): 2624-2626.
2. Takayoshi Ohtsu, Hitoshi Yoshida, and Noriaki Hat-anaka. *EOS / ESD Symposium Proceedings EOS-23* (2001): 173.
3. Takehiko Hamaguchi, Takayuki Ichihara, and Ta-kayoshi Ohtsu *EOS / ESD Symposium Proceedings EOS-24* (2002): 119.
4. Wallash, A, and Honda M. *EOS / ESD Proceedings EOS-19* (1997): 382-385.
5. Honda, M, and Nakamura Y. *EOS / ESD Proceedings EOS-9* (1987): 96-103.
6. Takayoshi, Ohtsu, and Shoji Natori. "Study on ESD / EMI Phenomena for Magnetic Reproducing Head". *IEEJ Trans Fund Mater.* 130 (2010): 473-478.
7. Takayoshi, Ohtsu, and kouji Kataoka. "Study on ESD Phenomena of Magnetic Head by 1ns Pulse ESD", *APEMC* (2010).
8. Takayoshi, Ohtsu. "Study on Robot Malfunction Due to Electrostatic Discharge", *25th RCJ Reliability Symposium* (2015): 84-87.

How to cite this article: Takayoshi Ohtsu, Yuma Nagao, Ryuji Ohsawa. "Analysis of Malfunction of Robot by ESD using Optical Electric Field Sensor." *J Biomed Syst Emerg Technol* S1 (2021): 001.